AIAA 82-4032

Vortex Model for Magnus Forces at Low Speeds, Spins, and Angles

Eugene E. Covert* and D. Scott Eberhardt†
Massachusetts Institute of Technology, Cambridge, Mass.

A slender body that is both spinning about its longitudinal axis and at an angle of attack experiences a force (and moments) whose plane of action is rotated 90 deg from the plane of the velocity vector and the longitudinal axis or spin axis of the body. This force (and moment) is called the Magnus force in honor of the discoverer. The results presented here show the nature of the Magnus force is strongly dependent upon whether or not vorticity is shed, and if shed, the coupling between the shed vorticity, spin induced effects, and the angle of attack.

Nomenclature

$a(x)$ = local radius of the body
C_N = normal force coefficient (referred to maximum body cross-sectional area)
C_Y = side force coefficient
d_{12} = distance between vortices
D = diameter (if not otherwise indicated, maximum diameter)
D_B = diameter at the base of a boat-tail body
ℓ_d = distance between separation point and vortex core
M = pitching moment
N = normal force
N = yawing moment
p = spin rate
t = time
r = radial coordinate
x = axial coordinate
U_x = axial velocity
U_r = radial velocity
U_θ = azimuthal velocity
U_∞ = freestream velocity
W = complex potential in cross flow plane
Y = side force
α = angle of attack
δ = local nose tangent angle with respect to body centerline
Θ = angular coordinate
Θ_{eq} = perturbed equilibrium separation point
Θ_{spi} = angular position of vortex feeding sheet spring point
Γ_i = circulation of ith vortex
ρ = air density
τ = cross flow characteristic time
Γ_X = strength of circulation of trailing vortex
κ = boattail effectiveness factor
ζ = complex coordinate in cross flow plane

Subscripts

i = 1, 2 refers to quantities associated with port and starboard trailing vortex, respectively
= 3 refers to the fixed central trailing vortex
WB = with boat-tail
SB = square base

Received Feb. 5, 1981; revision received Aug. 3, 1981.

*Professor of Aeronautics. Fellow AIAA.
†Graduate Student, Department of Aeronautics & Astronautics.

Introduction

THE aerodynamics of slender bodies spinning about their long axis and the production of Magnus force and moment has been the subject of three reviews in the last fifteen years.[1-3] The primary discussion in these reviews emphasized the importance of the boundary layer and its axial distribution in the development of the Magnus force[4] (cf., Appendix A). Next came detailed applications of boundary-layer theory.[5-7] Recently, finite-difference procedures have been used to couple the boundary layer to the outer flow.[8] These procedures are used for parametric studies, but are limited by the use of the boundary-layer theory assumptions. More basic studies using numerical solutions of the parabolized form of the Navier-Stokes equations[9] have indicated a possibility of overcoming some of these limitations.

Relatively little attention has been given to the reversed sign Magnus force in the small spin, small angle-of-attack region reported by Dietrick[10] from supersonic firing range data. This feature was confirmed by wind-tunnel tests reported by Platou and Sternberg.[11] They measured a reversed Magnus force in the BRL wind tunnel at a Mach number of 2 and a Reynolds number of 0.65×10^6. The body had a fineness ratio of 3.2. Its nose was a tangent ogive of a fineness ratio of 1.5, and its base was rounded to simulate the hemispherical base on Dietrick's model. A square base model with other similar geometry did not display the reversed sign Magnus force at the same wind-tunnel conditions. Later Fletcher[12] predicted a second class of reversed sign Magnus force. This class occurred at moderate angles of attack in the Reynolds number range where boundary-layer transition occurred on one lateral side of the body, but not on the other.

Recent experimental measurements at subsonic speeds[13-16] have also shown the existence of the first class of reversed sign Magnus force region at small values of reduced spin and small angles of attack with models having square or boat-tail bases. Rakich[17] has obtained a similar result by means of a numerical solution of the Navier-Stokes equations for small values of reduced spin and angle of attack, but at hypersonic Mach numbers.

In this paper an alternative fluid mechanical model to calculate Magnus forces is offered. The model is based upon vortex dynamics and uses experimental data for the vortex sheet spring point in each cross flow plane. In other words the intent is to describe or model key phenomena that combine to more or less explain observed variation of the Magnus force and moment.

Analysis

It has long been known that the normal force on a slender body is made up of two parts. First there is the classical cross flow linearized solution due to Munk. The force along the

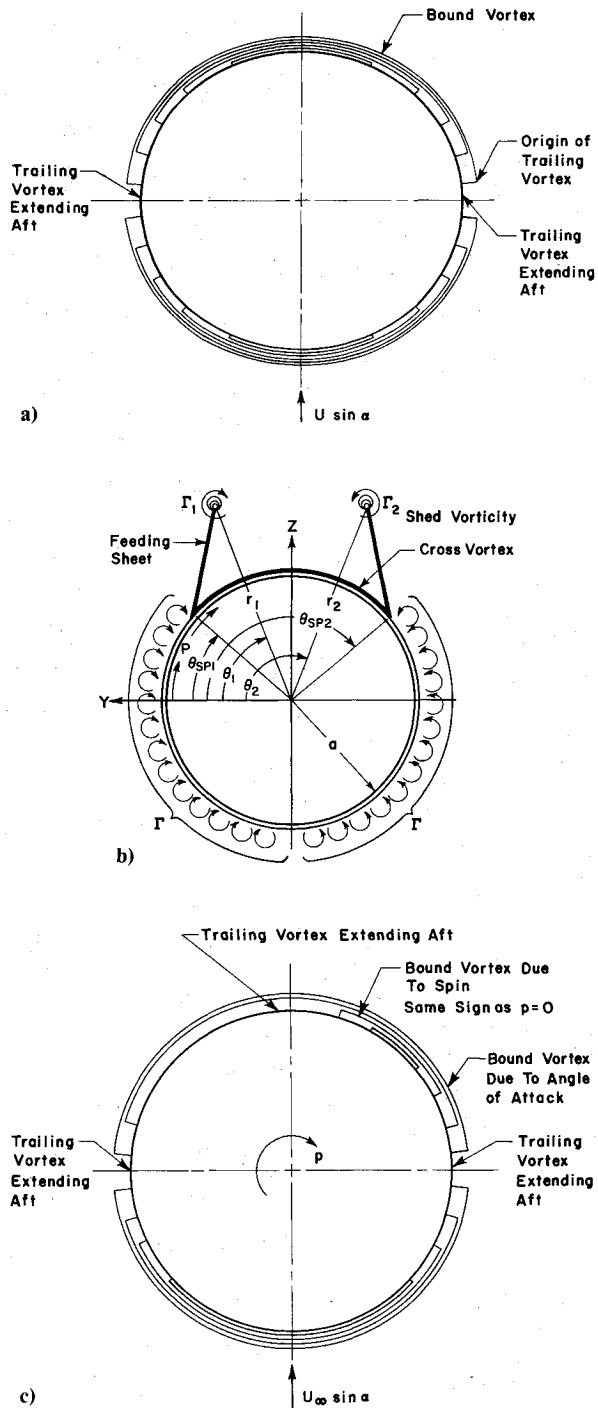

Fig. 1 a) Configuration of cross vortices (schematic), b) separated cross flow and c) configuration of cross vortices with spin.

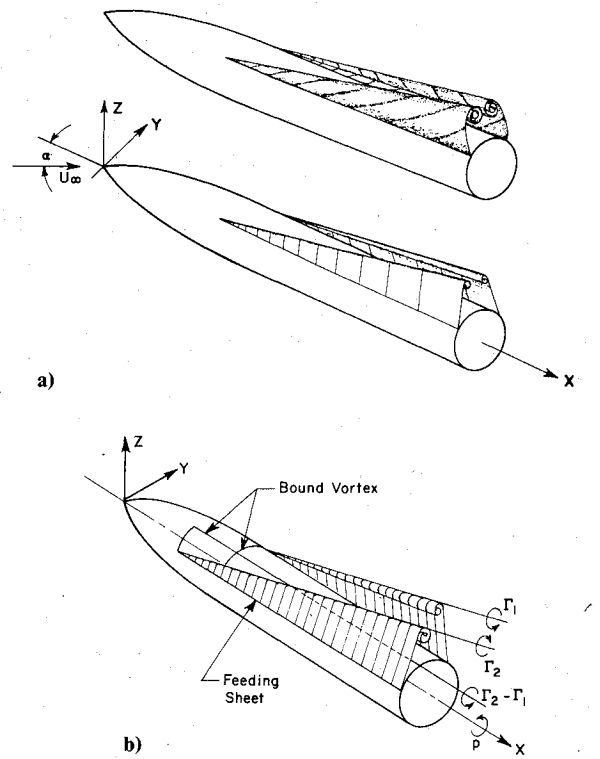

Fig. 2 a) Assumed actual separation of vortex sheet from the body, $p = 0$; b) approximate modeled configuration of shed velocity, $p = 0$.

body is also viewed as an unsteady change in the cross flow momentum. Hill[18] showed the Munk results could be derived from a cross flow vortex pattern (Fig. 1a). There is an additional force due to separated vorticity that was first calculated by Hill,[18] and was put on firmer ground by Bryson[19] and by Schindel.[20]

The flow model for the additional nonlinear normal force consists of azimuthal bound vortex elements making up the upper and lower surface of the body, a pair of vortex sheets that connect the body to a pair of concentrated vortex cores, and the vortex cores themselves. Figure 1b, shows Hill's sketch of his model in the cross flow plane. Note the vortex cores, the feeding sheets, and the angular position the springing points for the vortex sheet or feeding sheet are symmetrically located with respect to the plane defined by the longitudinal axis of the body and the velocity vector. These features are shown along with other geometry in Figs. 2a and 2b.

Subsequently, Schindel used a multiple vortex model in an attempt to treat the vortex sheet more realistically. Recently Mendenhall et al.[21] have constructed a more sophisticated model. Mendenhall[22] used source panels to represent the body, Stratford's separation criteria in the cross flow, and the usual vortex trajectory calculation. None of these models have been applied to study the flow past slender spinning bodies. In particular, the nature of the generalization of Stratford's separation condition to the case of a boundary layer on a moving wall is far from obvious.

In calculations of this type a key problem is that of identifying the locations of the point where the feeding sheet springs from the body. Both Hill and Schindel used experimentally observed data. Hill used an earliest position boundary-layer separation position, while Schindel used a position slightly further downstream that allowed for the complexity of the flow near the vortex sheet springing line. Sears[23] has shown that in laminar flow the separation point in an infinitely long swept cylinder is governed by the viscous cross flow and not by the flow along the generators. At the separation line the flow is turned to lie totally along the generators of the cylinder. Hence, if the body is assumed to be relatively slender, a not unreasonable assumption is made that the cross flow will determine the location of the spring line of the feeding vortex sheet. Mendenhall[22] has implicitly made this assumption when he used Stratford's separation condition. Sear's approach is also consistent with the unsteady cross flow idea that was cited earlier.

In this study, we will use the simple vortex modeling of Hill, Bryson, and Schindel. As Bryson pointed out[19] this model has at least two defects; angular momentum is not conserved, and the vortex trajectory approaches Föppl's no-force-locus. As a consequence of the latter characteristic the additive force can become zero for long bodies. The multiple vortex models appear to overcome this shortcoming of the single pair model. However, the added complexity seems to obscure some of the

physical processes of the flow past the spinning body. Hence, the simpler model was chosen. The expectation that the region of validity of the model would be reduced was realized.

There remains one issue in the approximation that has to be clarified. As long as $\Gamma_2 = -\Gamma_1$ it is clear vorticity is conserved. The basic element in Hill's model is that Γ_1 and Γ_2 represent the vorticity distributed on the surface between $\Theta_{sp1,2}$ and the aft stagnation point. Thus the total vorticity included in a circle that surrounds the body and shed vorticity is conserved since the change in increase in Γ_2 and reduction of Γ_1 merely represent a redistribution of the vorticity (Fig. 1b).

When the body is spinning the vortices separate non-symmetrically and move away at different rates. To ensure vorticity is conserved, a third vortex is added to the flow model (Figs. 1c and 2c). This vortex is located on the streamline passing through the upper midstagnation point and is connected via bound vortices to the stronger of the trailing vortices (Γ_1). Thus, we define $\Gamma_1 + \Gamma_3 = \Gamma_2$ for positive spin. So Γ_3 grows to conserve vorticity. The dynamics is simulated by fixing the location of Γ_3 near the body on the dividing streamline. Note that this model is roughly similar to the vorticity generated by a rolling wing of finite span, whose angle of attack is greater than zero. The most elemental model of this flow has two tip vortices plus one at the midspan.

Vortex Model

Assume for the moment the question of the angular location of the separation line is settled. The next step is the calculation of the vortex trajectory. It is defined by the no-force condition on the vortex and the feeding sheet,[18-20,24] viz.,

$$r_i \frac{d\Theta_i}{dt} = U_{\Theta_i} - \frac{U_x}{\Gamma_i}\frac{d\Gamma_i}{dx} r_i \sin(\Theta_i - \Theta_{spi}) \tag{1}$$

and

$$\frac{dr_i}{dt} = U_r + \frac{U_x}{\Gamma_i}\frac{d\Gamma_i}{dx}[r_i \cos(\Theta_i - \Theta_{spi}) - a] \tag{2}$$

$i = 1,2$ for the port and starboard vortex, respectively. r_i, Θ_i are polar coordinates of the ith vortex of circulation Γ_i (Fig. 1b). U_{Θ_i} and U_{r_i} are the azimuthal and radial velocity components at r_i, Θ_i and include the cross flow past the cylinder, the image of Γ_i (at a^2/r_i, Θ_i) and the other vortices and their image. Θ_{spi} is the coordinate of the separation line on the ith side (Fig. 1b). Note that

$$\frac{U_x}{\Gamma_i}\frac{d\Gamma_i}{dx} > 0 \tag{3}$$

The strength of the vortex is determined by the requirement that the point Θ_{spi} is a stagnation point.

The calculation of the forces is simplified by recalling that the pressure coefficient is proportional to the longitudinal derivative of the velocity potential. Hence the force up to a point is just the value of the potential at that point, which allows us to use the simplification offered by the complex potential and the well known momentum theorem of Blasius. Thus, if the complex potential for flow outside the boundary layer is $W(\zeta)$, the total forces acting on the cylinder up to station x are

$$N - iY = \frac{i}{2}\rho \oint \left(\frac{dW}{d\zeta}\right)^2 d\zeta \tag{4}$$

The details of this computation are straightforward and lead to

$$N = \rho U_\infty \sin\alpha\cos\alpha\left[\Gamma_1\left(r_1 - \frac{a^2}{r_1}\right)\cos\theta_1 + \Gamma_2\left(r_2 - \frac{a^2}{r_2}\right)\cos\theta_2\right] + \rho U_\infty^2 \cos\alpha\sin\alpha\pi a^2(x) \tag{5}$$

and

$$Y = -\rho U_\infty \sin\alpha\left[\Gamma_1\left(r - \frac{a^2}{r_1}\right)\sin\Theta_1 + \Gamma_2\left(r_2 - \frac{a^2}{r_2}\right)\sin\Theta_2\right] \tag{6a}$$

Note, for all practical purposes, Γ_3 can be omitted for this calculation since $r_3 \simeq a$. Similarly one can compute moments with respect to $x = 0$ in a straightforward way.

$$M = -N(x)x + \int_0^x N(x)\,dx \tag{6b}$$

and

$$N = Y(x)x - \int_0^x Y(x)\,dx \tag{6c}$$

Note, $M > 0$ implies nose up and $N > 0$ implies nose left.

Vortex Sheet Spring Point

To return to the problem of determination of Θ_{spi} and its sensitivity to spin about the long axis of the body, it is best to review the nature of the vortex springing line in new spinning flow. An approximation for a circular cylinder starting impulsively from rest and moving perpendicular to its long axis[26,27] shows that, in our cross flow notation, separation takes place after a time.

$$\tau = (x/D)\tan\alpha = 0.15 \tag{7}$$

In this result, due to Blasius, there is no separation at first, then the separation point starts at the rear stagnation point and moves forward toward the equilibrium value. Simple curve fitting suggests an approximation

$$\Theta_{spi} = \Theta_{spi}(0.15) \pm \sqrt{\frac{\tau - 0.15}{0.65}}\,(\Theta_{eq} - \Theta(0.15)) \quad \text{for } 0.15 < \tau < 0.7$$

$$= \Theta_{Eq} \quad \text{for } \tau > 0.7 \tag{8a,b}$$

Other apparent options, such as generalizing the work of Blasius, of Stratford, or of Moore[25] to include spin, or using Morton et al.[29] require additional research to make them useful. (Data given in Ref. 29 shows that to a first order in spin and in angle of attack the effects of spin are confined to the boundary layer. To this accuracy the measured cross flow velocity just outside the boundary layer agrees with the cross flow velocity based on potential theory. Note the configuration here is a hollow cylinder so there is little or no axial pressure gradient driving the external flow.) Hill assumed the measured cross flow separation line on a circular cylinder could be used. Bryson and Schindel assumed a tangent cone approximation and followed an idea of Moore.[25] He found a singularity with boundary-layer growth in flow past a slender

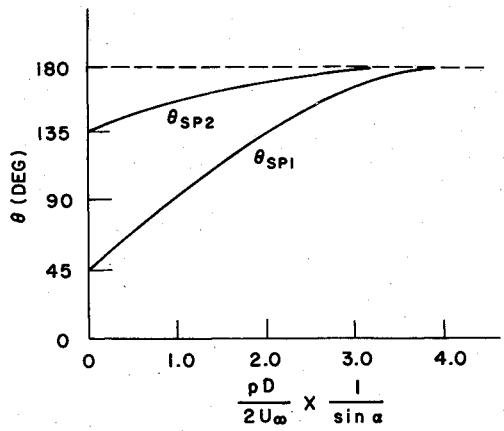

Fig. 3 Springing points as a function of spin rate.

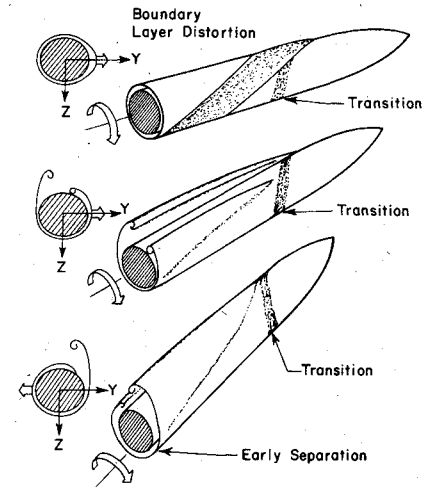

Fig. 4 Distortion of lee side vortex region due to spin at low, medium, and high angles of attack.

cone of half angle δ when the ratio

$$\tan\alpha/\tan\delta > 1.5 \tag{9}$$

It was assumed this singularity corresponded to the onset of separation. To allow for a spin, use Prandtl's photographs as reproduced by Goldstein[28] to represent the variation of the equilibrium value for Θ_{spi} as a function of spin (Fig. 3). Since we are using the simple vortex model, we followed Bryson and Schindel to define the angle of attack at which separation occurred by applying Eq. (9) locally on the nose to determine the start of the vortex. The effect of spin followed by using Fig. 3.

Calculation Procedure

Because of the suggestion that separation takes place on the nose, upstream of the cylinder, Eq. (9) was used to define the onset of separation. The initial conditions for Γ_i, r_i, Θ_i, were taken following Bryson[19] and Schindel.[20] The vortex trajectories were then found by integrating Eqs. (1) and (2). The forces and moments were found from Eqs. (5) and (6).

To summarize:

1) $\tan\alpha > 1.5 \tan\delta$ locally at start of vortex solution,‡ as modified by Fig. 3

2) Equations for the trajectory of the rolled-up vortex Eqs. (1) and (2) refer to Refs. 18-22

3) Potential flow is in the cross plane, including the cylindrical body, the vortices, and their images

4) The vortex strength was such that a stagnation point existed at the feeding sheet spring point. Note, by definition, $\Gamma_3 = \Gamma_2 - \Gamma_1$

5) The vortex position initially satisfies Bryson's conditon[19]; that is,

a) $\cos(\Theta_i - \Theta_{spi}) \simeq 1 - [(r/a) - 1]^2$.

b) $\Gamma_i = 2\cos\Theta_{spi}[(r/a) - 1]2U_\infty \pi a$.

c) The feeding sheet is 30 deg above the tangent, which fixes Θ_i.

d) r/a was selected at 1.005 for $i = 1$, 2, and 3.

Note that these conditions are not too critical. Errors in the initial condition seem to be integrated out in the first 1-2% of the body length.

6) The forces were computed using momentum integral.

Discussion

A number of interesting results follow without difficulty. Consider the relation to the boundary condition at Θ_{spI} as spin increases. As Θ_{spI} approaches 90 deg (Fig. 4) the external potential flow approaches a stagnation point. Hence, the strength of Γ_I needed to cancel the cross flow becomes smaller. Eventually vortex (1) will not be measurable but vortex (2) in the starboard or counter-rotating side remains. Martin and Ingram's results,[13] reproduced here in Fig. 4, show this effect dramatically. This also agrees with measured results.[30]

Furthermore, Eqs. (1) and (2) imply that for small reduced spin, the tendency for Θ_{spi} to move in the spin direction causes the vortex to move in the spin direction faster than it moves radially (Fig. 5a). From Eq. (5) we see N is unaltered to a first order, but that increasing Θ_1 and Θ_2 somewhat, while holding Γ_1, $\Gamma_2 (\simeq -\Gamma_1)$, r_1 and r_2 constant, implies a force in the $-y$ direction or contrary to that expected, as shown by the relation

$$C_Y = -2\frac{\Gamma}{U_\infty \pi a}\sin\alpha\left(\frac{r_I}{a} - \frac{a}{r_I}\right) \times \left(\frac{\partial\Theta_{spI}}{\partial\left(\frac{pD}{2U_\infty}\right)} + \frac{\partial\Theta_{sp2}}{\partial\left(\frac{pD}{2U_\infty}\right)}\right)\frac{pD}{2U_\infty} \tag{10}$$

While this force is in the correct direction its magnitude is too small by roughly a factor of 10.§ For larger spin $\Gamma_I \to 0$ when $\Theta_{spI} \to \pi/2$ implies the side force, $Y > 0$; i.e., a force in the expected direction.

From a different point of view, in the first case of low spin, the vortex pattern tends to rotate in the spin direction and hence the downwash has a $+y$ component or a $-Y$ force.

‡The idea of an off-on type of initiation of separation is clearly too simple, but it appears more detailed solutions than are currently available are needed to provide greater precision.

§It should be noted that at these low angles of attack the vortex pair move more or less parallel to the body. The initial condition ($r/a = 1.005$) is sufficient to clear the boundary layer. However, at the base of the body the boundary layer is sufficiently thick that the implicit assumption of a noninteracting vortex and boundary layer is probably invalid. If one includes the axial displacement thickness in the calculation, the incremental vortex motion more than doubles, which increases the strength of the vortex, in turn. Hence, the factor of 10 is reduced to between 2.5 and 3 by this procedure. However, the vortex and boundary layer would seem to be so closely coupled that an ad hoc procedure allowing for the boundary-layer effect on the vortex trajectory without allowing for the effect of the vortex on the boundary layer is difficult to justify, and hence was not used. Longitudinal vortices have been measured in boundary layers.[27,31] Similar observations have been made in by-flow visualization by F. N. M. Brown at Notre Dame.

Table 1 Proper sign Magnus data

Source	M	$Re\times10^{-6}$	L/D	$\left.\frac{L}{D}\right\|_{AB}$ [a]	$\frac{dC_Y}{d\left(\frac{pD}{2U_\infty}\right)}$ $\alpha=7.5$ deg	Remarks
Ref. 15, Fig. 8.3	0.2	0.77	7	5	0.19	Square base, smooth model
Ref. 15, Fig. 8.4	0.2	0.77	7	5	0.32	Square base, rough model
Ref. 14, Fig. 11	0.2	0.76	5	3.5	0.28	Square base, rough model
Ref. 14, Fig. 6a	0.2	0.76	5	3.5	0.12	Square base, smooth model
Ref. 13, Fig. 1	0.07	0.94	7	5	0.32	Square base, $\alpha=10$ deg
Ref. 1, Fig. 5[b]	2	0.168	3	1.5	0.008	Rounded base, roughness added ($\alpha=5$ deg)
Ref. 16, Fig. 17		0.315	6	3.0	0.14	7 deg D conical boat-tail
Fig. 18		1.03	6	3.0	0.25	square base

[a] Afterbody fineness ratio. [b] Corrected to a square base, for area ratio 1, the slope takes the value 0.08.

This may be demonstrated by computing the radial average of axial circulation in the annulus at a constant lengthwise position. To a first order in reduced spin the average axial circulation is independent of azimuth. This implies the fluid pattern tends to rotate as a whole.

However, at large spin, the fact that (Γ_2) is larger than (Γ_1) implies that the vortex pair tends to rotate in the counter-spin direction at a rate ω.

$$\omega=\frac{\Gamma_2+\Gamma_1}{2\pi d_{12}^2} \qquad \Gamma_1>0,\quad \Gamma_2<0 \text{ and } \omega<0 \qquad (11)$$

This is in a direction to cause the downwash to be in the $-y$ direction implying a $+y$ force, as expected (Fig. 5b).

Equation (6) implies the Magnus force due to the shed vorticity is dependent primarily on the distance the vortex pair has moved outward, which is roughly proportional to the length of the body after separation, or approximately the length from the start of the cylindrical body. The data in Fig. 6 and in Table 1 suggest that this length is reasonably good for correlating existing data. The table also shows that the effect of roughness to trip the boundary layer is an important factor, or that Θ_{spl} is sensitive to the boundary-layer state, a factor not included in our model because of a lack of information on the effects of the moving wall on location of the vortex spring point when the boundary layer is turbulent.

As mentioned earlier, Bryson[19] has shown that the vortex model predicts the unsteady load accurately at early times but loses accuracy as the vortex approaches the zero force locus. At higher spin the vortex on the corotational side starts close to the zero force locus. Hence, the inaccuracy should appear early on. Examination of Fig. 7a shows that this is indeed true. The calculated value of C_Y and C_N compare well with Birtwell's data[14] up to $pD/2U_\infty\simeq0.075$; then the magnitude of C_Y falls off. This fact is recognized by limiting the region of validity of our model to $(pD/2U_\infty)<\frac{1}{2}\sin\alpha$. (Note at $\alpha=10$ deg, $pD/2U_\infty=0.1$ the weak vortex is becoming very weak indeed.)

Birtwell's Fig. 6a shows C_Y is nearly zero for reduced spin up to 0.15 if the angle of attack is 5 deg. The calculated value at 5-deg angle of attack is $P=0.025$, 0.05, and 0.075; $C_Y=-0.0002$, -0.0001, and 0.0001. This value is approximately zero and tends to confirm Birtwell's measurements.

Figure 7b shows the variation of C_Y with α at a reduced spin of 0.045. The vortex model seems to be a reasonable estimate for $\alpha>5$ deg. At lower values of α the sign is correct, but the magnitude is wrong, as discussed earlier following Eq. (10).

A comparison with Henderson's data[15] is shown in Fig. 8 for $\alpha=6$ deg. Since the body is much longer, one expects the range of spin for which the calculation is valid to be reduced, as is indeed the case.

Finally, the comparison with the data of Kegelman et al.[16] is shown in Table 2.

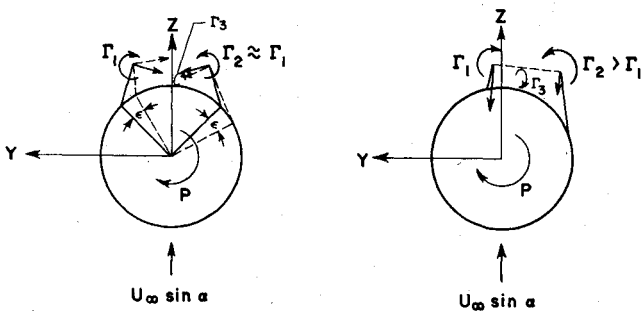

Fig. 5 a) Small spin b) larger spin.

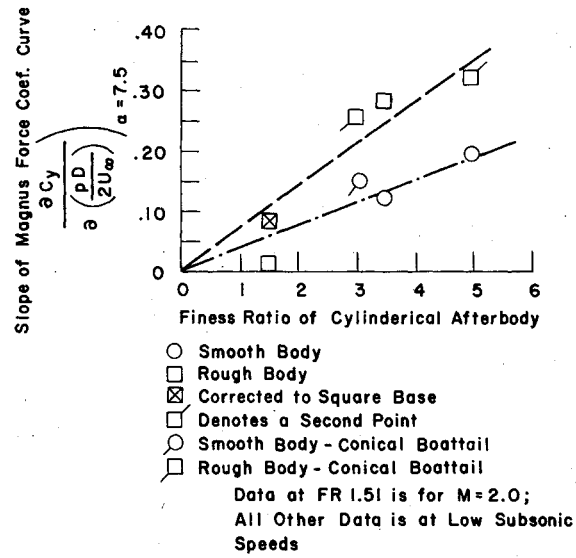

Fig. 6 Initial slope of Magnus force coefficient curve.

Table 2 Comparison with data of Ref. 16

$\alpha = 7.5$ deg			Re
P	0.025	0.050	
$C_{Y_{calc}}$	0.0104	0.0171	
$C_{Y_{meas}}$	0.009	0.015	0.315×10^6
	0.006	0.012	1.03×10^6

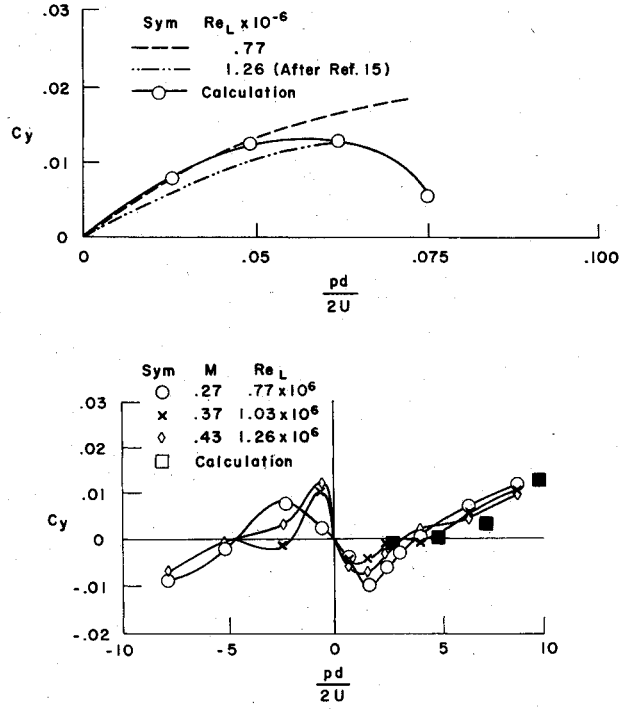

Fig. 7 a) Reynolds number effect C_Y vs $pD/2U_\infty$, $\alpha = 9.5$; b) side-force coefficient vs α at $pD/2U_\infty = 0.0450$ (fineness ratio 5).

The data in Ref. 16 are for a body with a boattail. The agreement including this complication seems surprising; but for a boattail, it is possible to make the same argument at low values of angle of attack as made before. The spin-induced rotation of the separation line leads in this case to a positive side force coefficient because of the negative lift on a boattail. Further, the boundary layer is relatively thick on the boattail compared to the nose, so the effect of the spin may be more pronounced. Nevertheless, flow separation would reduce the size of the effect.

The results for the small rounded corner at subsonic speeds (Table 1) seem to be anomalous. However, the degree of rounding is comparable to the boundary-layer thickness in magnitude. Thus, a change in flowfield could be due to much more subtle phenomena than those under discussion. For the present, this point remains enigmatic. Another enigma is the effect of the sting reported in Refs. 14 and 15, and the effect of roughening the body, which seems to increase the value of the incremental side force due to the base. The data in Refs. 3 and 15 show that a cavity in the base has a large, unexpected influence. The reason for such behavior cannot be explained simply by the vortex model. Because of the difficulty in dealing with separation simply, and because of the lack of data, these enigmas will be pursued no further.

Closing Remarks

This model suggests the origin of the Magnus force is more complex than previously expected. There seem to be at least three distinct phenomena. The first phenomenon is in the angle of attack and spin range for which there is no vortex separation. Here the boundary layer calculation of Martin,[4] as generalized by his co-workers,[5-8] is applicable. This situation gives a Magnus force and moment of the expected sign. The second phenomenon is the unexpected reverse sign contribution due to the weak vortex separation that is rotated in the spin direction. This flow is governed by a more complicated process than the simple vortex model, although the simple model predicts a reverse sign domain. The third is the consequence of unequal separation and vortex strength that gives the expected sign to the Magnus force. The primary role that the boundary layer plays is in its effect upon the separation line or vortex sheet spring point, which so far has been based on empirical data, rather than based upon "first principles." Figure 9 shows these regions as elements in a three-dimensional zone.

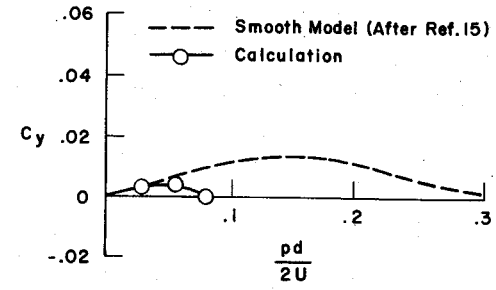

Fig. 8 Magnus force coefficient 7:1 fineness ratio body ($\alpha = 6$ deg).

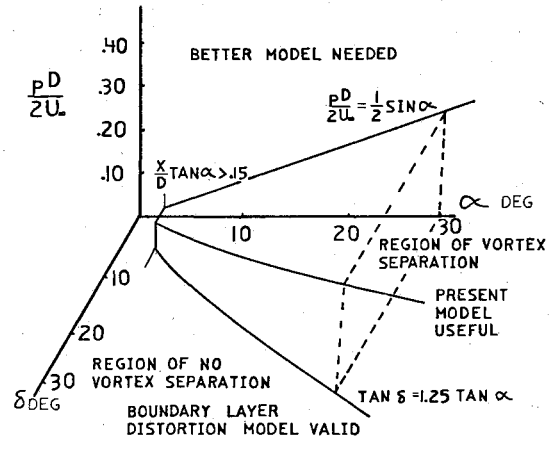

Fig. 9 Regions of usefulness of different models.

Further progress in understanding of the origin of the Magnus force would seem to rest upon 1) better understanding of the location of the vortex spring line as a function of the geometry and state of the boundary layer; 2) better understanding of the interaction of the vorticity and the boundary layer in the low (0-5 deg) angle-of-attack range; and 3) better understanding of the influence of the base on Magnus forces and moment. It is difficult to imagine how this can come about with downstream marching type solutions since the base effect seems to be an upstream coupling.

Appendix—Historical Comments

In the classic model for the calculation of the Magnus force acting on a slender body at small angles of attack (see Fig. 2), the fluid is assumed to be incompressible and inviscid. Thus, the flow can be determined by use of potential flow solutions of Laplace's equation. The cross flow velocity in the $+z$ direction is

$$U_\infty \sin\alpha \simeq U_\infty \alpha \qquad \text{(A1)}$$

The spinning is accounted for by equating the peripherical velocity at the cylinder due to spin rate (p) with that induced

by a vortex (which extends from the nose of the body downstream; in the $+x$ direction). For a very slender body the vortex is semi-infinite. Thus,

$$U_\theta = \frac{pD}{2} = \frac{2\Gamma}{4\pi D} \tag{A2}$$

Thus, the circulation may be found to be

$$\Gamma = \pi p D^2 \tag{A3}$$

The force per unit length is

$$Y = \rho U_\infty \sin\alpha \Gamma = \rho U_\infty \sin\alpha p \pi D^2 \tag{A4}$$

The Magnus force coefficient, with the base area of the cylinder used as the reference area is

$$C_Y = 8\alpha \frac{pD}{2U_\infty} \frac{L}{D} \tag{A5}$$

Here the length of the body more or less in the flow direction is L.

This formula shows a linear dependence of the Magnus force upon the angle of attack and the reduced spin rate of the body. Except for the power of the fineness ratio, the result from this simple model seems to be functionally correct at high spins and moderate angles of attack. However, the simple model raises conceptual difficulties. Using boundary-layer theory one can account for the effects of viscosity on the inner flow along with a potential outer flow. This more complex model indicates the effect of viscosity vanishes at the outer edge of the boundary layer. How then is the effect of the spin communicated to the outer flow? To answer this question, apply another concept in fluid mechanics that results in the simple model. This is the relation between circulation and vorticity. If one models the body with distributed vorticity,[18] the axial flow sees a vorticity made up of a distribution of vortex rings, and the cross flow sees a family of vortex lines lying on the surface and extending in the x direction. If the cross flow is in the $+z$ direction ($\phi = \pi/2$) and if theta is measured from the y direction the cross flow sees a distribution of vorticity

$$\gamma = 2U_\infty \sin\alpha \sin(\phi - \theta) \tag{A6}$$

which is the jump in velocity across the vortex sheet. (Note: Prandtl has shown for a model of this kind that the flow is stationary on the inside vortex sheet, thus the pressure inside the vortex sheet is just total pressure.) With these ideas as a background, another approximation suggests itself. Namely, instead of using a zero velocity at the wall, one uses U_θ defined earlier. Thus, one now obtains in a no less rigorous way the vorticity distribution across the layer with spin

$$\gamma = 2U_\infty \sin\alpha \sin(\phi - \theta) + pD/2 \tag{A7}$$

Note, now the vorticity is increased on the positive y side of the body, and is reduced on the negative y side. The stagnation points, where the vorticity and velocity are zero, now occurs at

$$\phi - \theta = -\sin^{-1}\frac{pD}{4U_\infty \sin\alpha}; \quad \pi + \sin^{-1}\frac{pD}{4U_\infty \sin\alpha} \tag{A8}$$

instead of zero and π.

If one integrates the product of the vorticity and the longitudinal velocity component over the area of body,¶ one finds a lift coefficient (assuming a pointed nose)

$$C_L = \sin 2\alpha \tag{A9}$$

and a side force coefficient

$$C_Y = 16 \sin\alpha \frac{pD}{2U_\infty} \frac{L}{D} \int_0^L \frac{r(x)}{r_{\max}} \mathrm{d}\left(\frac{x}{L}\right) \tag{A10}$$

The latter is a slight generalization of the results obtained before, but an alternate way of viewing the interaction makes itself clear. The effect of the spin makes itself felt through an asymmetry of the cross flow.

This view is physically consistent with the idea that spin would distort the boundary layer, and hence, of the apparent shape of the body. This implies a nonuniform distribution of the displacement thickness. Martin[4] solved the problem of the boundary layer on a slender spinning body at a small angle of attack. He found the distribution was no longer axially symmetric. Then he computed the displacement thickness distribution ($\delta^*(x)$). As expected this caused an apparent camber in the yaw plane, and thus a Magnus force; namely,

$$C_Y = 30.6\alpha \frac{pD}{2U_\infty} \frac{L}{D} \frac{\delta_{D^*}}{D} \tag{A11}$$

The result is functionally the same as before, except for a nonlinear dependence upon the fineness ratio that is due to the linear dependence of δ^*/D upon fineness ratio, to wit

$$\frac{1.7}{\sqrt{Re_L}} \frac{L}{D} \quad \text{laminar flow}$$

$$\frac{C'}{(Re_L)^{0.2}} \frac{L}{D} \quad \text{turbulent flow} \tag{A12}$$

Since Martin's result is in much better agreement with experiment than the simple model, one must conclude that the boundary layer must be included in the solution in a less desiccated way than in the vortex model with only a jump in velocity across the surface. Martin's model is asymptotically valid for low α and low spins[4] and seems to be useful at higher angles of attack[5,6] where it predicts the same magnitude as the simple vortex model.

¶The details of this calculation have been carried out for $p = 0$ in Ref. 18.

Acknowledgments

This study was primarily supported by the Army Research Office under Contract DAAG29-75-C-0001; Dr. Robert Singleton was Project Monitor.

References

[1] Platou, A. S., "Magnus Characteristics of Finned and Unfinned Projectiles," *AIAA Journal*, Vol. 3, Jan. 1965, pp. 83-90.

[2] Regan, F. J., "Magnus Effects," *Fluid Dynamic Aspects of Ballistics*, AGARD CP 10, Sept. 1966, pp. 291-318.

[3] Jacobson, I. D., "Magnus Characteristics of Arbitrary Rotating Bodies," AGARDograph 171, Nov. 1973.

[4] Martin, J. C., "On Magnus Effects Caused by Boundary Layer Displacement Thickness in Bodies of Revolution at Small Angles of Attack," *Journal of the Aeronautical Sciences*, Vol. 24, No. 6, 1957, pp. 421-429; also, BRL Report 870, U. S. Army Ballistic Research Laboratories, Aberdeen Proving Ground, Md., June 1955 (revised).

[5] Vaughn, H. R. and Reis, G. E., "A Magnus Theory for Bodies of Revolution," *AIAA Journal*, Vol. 11, Nov. 1973, p. 1396.

[6] Dwyer, H. A. and Sanders, B. R., "Magnus Forces on Spinning Supersonic Cones, Part I. The Boundary Layer," *AIAA Journal*, Vol. 14, April 1976, pp. 498-504.

[7] Lin, T. C. and Rubin, S. G., "Viscous Flow over Spinning Cones at Angle of Attack," *AIAA Journal*, Vol. 12, April 1974, pp. 975-985.

[8] Sturek, W. S., Mylin, D. C., and Bush, C. C., "Computational Parametric Study of the Aerodynamics of Spinning Slender Bodies at Supersonic Speeds," AIAA Paper 80-1585, Aug. 1980.

[9] Sturek, W. B. and Schiff, L. B., "Computation of the Magnus Effect for Slender Bodies in Supersonic Flow," AIAA Paper 80-1586, Aug. 1980.

[10] Deitrick, R. E., "Effect of a Hemispherical Base on the Aerodynamic Characteristics of Shells," Ballistic Research Laboratories, BRL Report 947, Nov. 1955.

[11] Platou, A. S. and Sternberg, J., "The Magnus Characteristics of a 30 mm Aircraft Bullet," Ballistic Research Laboratories, BRL Report 994, Sept. 1956.

[12] Fletcher, C. A. J., "Negative Magnus Forces in the Critical Reynolds Number Regime," *Journal of Aircraft,* Vol. 9, Dec. 1972, pp. 826-833.

[13] Martin, J. M. and Ingram, C. W., "Experimental Correlation between the Flow and Magnus Characteristics of a Spinning Ogive-Nose Cylinder," *AIAA Journal,* Vol. 11, July 1973, pp. 901-902; synoptic of a Ph.D. Thesis by J. M. Martin, University of Notre Dame, 1971.

[14] Birtwell, E. P., "Magnus Forces and Sting Interference on Magnetically-Suspended Ogive Cylinders," Thesis submitted to the Department of Aeronautics and Astronautics, M.I.T. for S.M. degree, May 1974; see also, Birtwell et al., *AIAA Journal,* Vol. 16, Feb. 1978, pp. 111-116.

[15] Henderson, R. I., "The Use of a Magnetic Suspension Balance for the Measurement of Aerodynamic Magnus Forces on a Body of Revolution," S. M. Thesis, University of Southhampton, England, June 1976.

[16] Kegelman, J. T., Nelson, R. C., and Mueller, T. J., "Boundary Layer and Side Force Characteristics of a Spinning Axisymmetric Body," AIAA Paper 80-1584, Aug. 1980.

[17] Rakich, J. V. and Agarwal, R., "Computation of Hypersonic Viscous Flow Past Spinning Sharp and Blunt Cones at High Angles of Attack," AIAA Paper 78-65, Jan. 1978.

[18] Hill, J. A. F., "A Nonlinear Theory of Lift on Slender Bodies of Revolution," U. S. Navy Symposium on Aeroballistics at the Applied Physics Laboratory, The Johns Hopkins University, Silver Spring, Md., Oct. 1954.

[19] Bryson, A. E., "Symmetric Vortex Separation on Circular Cylinders and Cones," *Journal of Applied Mechanics,* Vol. 26, Dec. 1959, p. 644.

[20] Schindel, L. H., "Effect of Vortex Separation on the Lift Distribution of Bodies of Elliptic Cross Section," *Journal of Aircraft,* Vol. 6, Nov.-Dec. 1969, pp. 537-543.

[21] Mendenhall, M. R., Spangler, S. B., and Perkins, S. C. Jr., "Vortex Shedding from Circular and Non-circular Bodies at High Angles of Attack," AIAA Paper 79-0026, Jan. 1979.

[22] Mendenhall, M. R., "Predicted Vortex Shedding from Non-Circular Bodies in Supersonic Flow," AIAA Paper 80-1559, Aug. 1980.

[23] Sears, W. R., "The Boundary Layer of Yawed Cylinders," *Journal of the Aeronautical Sciences,* Vol. 15, Jan. 1948, pp. 49-52.

[24] Edwards, R. H., "Leading Edge Separation from Delta Wings," *Journal of the Aeronautical Sciences,* Vol. 21, No. 2, 1954, pp. 134-135.

[25] Moore, F. N., "Displacement Effect of a Three-Dimensional Laminar Boundary Layer Flow," *Journal of the Aeronautical Sciences,* Vol. 20, No. 8, 1953, pp. 525-534.

[26] Rosenhead, K. E., *Laminar Boundary Layers,* Oxford at the Clarendon Press, 1963, pp. 368-376.

[27] Schlicting, H., *Boundary Layer Theory,* 7th ed., McGraw Hill, New York, 1979, pp. 415-425, 530.

[28] Goldstein, S., ed., *Modern Development in Fluid Dynamics,* Dover, New York, Vol. I, Plate 17.

[29] Morton, J. B., Jacobson, I. D., and Saunders, S., "Experimental Investigation of the Boundary Layer on a Rotating Cylinder," *AIAA Journal,* Vol. 14, Oct. 1976, pp. 1450-1463.

[30] Finn, D. M., "Wake Measurements behind a Magnetically-Suspended Spinning and Non-Spinning Ogive Cylinder at Angles of Attack," M.I.T. Dept. of Aeronautics, S. M. Thesis, Feb. 1976.

[31] Morrisettes, E. L. and Bushnell, D. M., "Evidence of Imbedded Vortices in a Three-Dimensional Shear Flow," *AIAA Journal,* Vol. 10, March 1981, pp. 400-402.